Effect of Viscosity on the Equilibrium Scour Depth at Single Cylindrical Piers

Rui M. M. Lança[1]; Gonzalo Simarro[2]; Cristina M. S. Fael[3]; and António H. Cardoso[4]

Abstract: Most studies on scouring seem to have overlooked the effect of viscosity, the assumption being that the flow is free of viscous effects inside the scour hole because of the presence of highly turbulent flow structures such as down-flow, horseshoe vortex, and wake vortices irrespective of the approach flow regime. The present work reports the results of experiments conceived to revisit the effect of viscosity on scouring. The experiments were performed by changing the Reynolds-like numbers for two flow shallowness values and keeping constant the remaining dimensionless parameters that control the scour process. The values of the Reynolds number corresponded to transitional approach flows. The experimental results indicate that scouring does depend on viscosity in usual laboratory conditions, the viscous effect leading to scour depths in the safety side. **DOI: 10.1061/(ASCE)HY.1943-7900.0001102.**

Author keywords: Local scour; Viscosity; Cylindrical pier.

Introduction

Local scour at bridge piers has been studied over decades, mostly through experimentation. The early research works of Shen et al. (1969), Nicollet and Ramette (1971), Coleman (1971), and Monti (1994) seem to indicate that viscosity effects the equilibrium scour depth. According to Shen et al. (1969), the equilibrium scour depth depends on the pier Reynolds number, R_p ($=UD_p/\nu$, with U = mean approach velocity, D_p = pier diameter, and ν = kinematic molecular viscosity), because the size and strength of the horseshoe vortex, which is a key agent of the scouring process, depends on the Reynolds number. As stated by Shen et al. (1969), the equilibrium scour depth increases with R_p for constant sediment coarseness (D_p/D_{50}, with D_{50} = median sediment size) up to a certain limit, and when more than the limit, it decreases with the same nondimensional parameter. The experiments reported by Shen et al. (1969) cover the range $2 \cdot 10^4 \leqslant \mathsf{R}_p \leqslant 2 \cdot 10^5$. Nicollet and Ramette (1971) characterized the effect of the approach-velocity sediment Reynolds number R_s ($=UD_{50}/\nu$) and sediment coarseness ($=D_p/D_{50}$) on the equilibrium scour depth and reported that it decreases with R_s for $50 \leqslant \mathsf{R}_s \leqslant 5 \cdot 10^4$. Coleman (1971) concluded that scouring is independent from the pier Reynolds number for $\mathsf{R}_p > 10^4$ and Monti (1994) suggested that the scouring process is free of viscous effects if $\mathsf{R}_p > 7 \cdot 10^3$.

Reynolds number influences the size and strength of the horseshoe vortex and the frequency and strength of the wake vortices shed from piers. According to Ettema et al. (2006), small cylinders generate wake vortices of great vorticity. As the cylinder diameter increases, the power associated with the peak frequency of shed eddies decreases, reducing the relative scouring capacity of wake vortices and the dimensionless equilibrium scour depth. In practice, experimental research on scouring based on small size piers is claimed to produce unrealistically high values of dimensionless scour depth because of an inadequate similitude of large-scale turbulence. Ettema et al. (2006) also state that "Reynolds number in terms of viscous effect is unlikely to have direct bearing on scour depth." This can be understood as if the type of approach flow (rough turbulent or transitional) was irrelevant in the scour process, but implicitly leaving open the possibility that the flow structures associated with the pier (stagnation in the pier nose, downflow, internal boundary layer along the pier lateral walls, and the wake vortices detaching from the pier) depend on viscosity. This would be true even in the cases were the approach flow is rough turbulent because the flow structures associated with the pier are local phenomena.

In spite of the exceptions discussed previously, most of the literature regarding local scour in the past decades disregards the viscous effects, assuming that the flow structures around the pier are highly turbulent. The purpose of this work is to analyse the influence of the viscosity on scouring in current laboratory conditions. This is achieved through the discussion of the outputs of eight experiments conceived to isolate the effect of the viscosity on scouring.

Framework for Analysis

We consider the equilibrium scour depth, d_{se}, for a cylindrical pier under steady uniform flow conditions. The equilibrium scour depth around cylindrical piers inserted in uniform and fully developed flows in wide rectangular channels whose bed is composed of uniform nonripple-forming sand depends on the gravitational acceleration, g, water properties (density, ρ, and kinematic molecular viscosity, ν), sediment properties (density, ρ_s, and median size, D_{50}), flow (upstream undisturbed depth averaged velocity, U, and water depth, d), and the pier diameter, D_p. Given its physical interest, the critical velocity, U_c, defined as the depth averaged velocity for the threshold condition of sediment entrainment, is often considered in the analysis, so that we write

[1]Professor, Departamento de Engenharia Civil, Instituto Superior de Engenharia, Universidade do Algarve, Campus da Penha, 8005-139 Faro, Portugal (corresponding author). E-mail: rlanca@ualg.pt

[2]Associate Researcher, ICM-CSIC, Passeig Marítim de la Barceloneta 37-49, E-08003 Barcelona, Spain. E-mail: simarro@icm.csic.es

[3]Assistant Professor, C-MADE & UBI, Universidade da Beira Interior, Calçada Fonte do Lameiro, 6200-358 Covilhã, Portugal. E-mail: cmsf@ubi.pt

[4]Full Professor, CEris/Cehidro, Instituto Superior Técnico, Universidade de Lisboa, Av. Rovisco Pais 1, 1049-001 Lisboa, Portugal. E-mail: antonio.cardoso@tecnico.ulisboa.pt

Note. This manuscript was submitted on February 11, 2015; approved on September 13, 2015; published online on November 4, 2015. Discussion period open until April 4, 2016; separate discussions must be submitted for individual papers. This technical note is part of the ***Journal of Hydraulic Engineering***, © ASCE, ISSN 0733-9429.

$$d_{se} = f(g,\rho,\nu,\rho_s,D_{50},U,d,D_p,U_c) \quad (1)$$

where f stands for function of.

In this context, wide channels are those whose wall and contraction effects are negligible. Uniform, nonripple-forming sand is defined by $\rho_s \approx 2{,}660\,\mathrm{kg/m^3}$, $D_{50} \geq 0.6$ mm, and $\sigma_D < 1.5$, with σ_D = gradation coefficient of the sand. Fully developed flows are not necessarily rough flows. They are transitional flows in most of the experimental studies on scouring, as shown by Simarro et al. (2007). It will be further assumed that the sediment density, ρ_s, plays its role inasmuch as it contributes to the submerged sediment weight, so that it is replaced by $g(\rho_s - \rho)D_{50}^3$, to get

$$d_{se} = f[g,\rho,\nu,g(\rho_s - \rho)D_{50}^3,D_{50},U,d,D_p,U_c] \quad (2)$$

Applying the Vaschy-Buckingham theorem and assuming that $\Delta \equiv \rho_s/\rho - 1$ is constant, we get, among other expressions

$$d_{se}/D_p = f(d/D_{50},d/D_p,F_{c50},d_*,F_{50}) \quad (3)$$

$$d_{se}/D_p = f(d/D_{50},d/D_p,F_{c50},d_*,\mathcal{I}) \quad (4)$$

where $d_* = \sqrt[3]{g\Delta D_{50}^3/\nu^2}$; $F_{c50} \equiv U_c/\sqrt{g\Delta D_{50}}$; $F_{50} \equiv U/\sqrt{g\Delta D_{50}}$; and finally $\mathcal{I} \equiv U/U_c$ is the flow intensity.

The critical velocity, however, does not introduce any additional information relative to the rest of variables in the right hand side of Eq. (2), because

$$U_c = f[\rho,\nu,g(\rho_s - \rho)D_{50}^3,D_{50},d] \quad (5)$$

and all the variables in the right hand side of Eq. (5) are already present in the right hand side of Eq. (2). Applying the Vaschy-Buckingham theorem to Eq. (5)

$$f(d/D_{50},F_{c50},d_*) = 0 \quad (6)$$

Eq. (6) shows that three of the groups in Eqs. (3) and (4) are linked and, thus, one of them (d/D_{50}, F_{c50} or d_*) is to be deleted —d_* only if it plays a role in Eq. (6), i.e., if U_c depends on the viscosity. For example, deleting d_* from Eq. (4) we get

$$d_{se}/D_p = f(d/D_{50},d/D_p,F_{c50},\mathcal{I}), \quad (7)$$

but also, noting that $F_{c50}\mathcal{I} = F_{50}$

$$d_{se}/D_p = f(d/D_{50},d/D_p,F_{50},\mathcal{I}) \quad (8)$$

Alternatively, deleting F_{c50} from Eqs. (3) and (4) we get

$$d_{se}/D_p = f(d/D_{50},d/D_p,d_*,F_{50}) \quad (9)$$

$$d_{se}/D_p = f(d/D_{50},d/D_p,d_*,\mathcal{I}), \quad (10)$$

and, manipulating Eq. (9)

$$d_{se}/D_p = f(d/D_{50},d/D_p,\mathsf{R}_p,F_{50}) \quad (11)$$

Because our goal is to investigate if common laboratory experiments are influenced by viscous effects, it is necessary that the viscosity appears in only one dimensionless group. This is the case for Eqs. (8), (9), and (11), where the viscosity is represented repectively through $\mathcal{J}$, d_* and R_p. Conversely, recalling that, in general, U_c depends on ν, there are two viscous-dependent groups in Eqs. (7) and (10).

Departing from the framework given by the Eqs. (8), (9) and (11), the tests reported here consist in two sets designed so as to keep, within each set, d/D_{50}, d/D_p and F_{50} constant (*i.e.*, imposing Froude similarity) and to vary the viscosity-dependent numbers $\mathcal{J}$, d_*, and R_p. Actually, showing that Eq. (8) depends on $\mathcal{J}$ is equivalent to show that Eqs. (9) and (11) depend respectively on d_* and Re_p, and equivalent to show that d_{se} depends on the viscosity ν.

Experiments

Experiments were carried out in the 28.0-m long, 4.00-m wide, and 1.00-m deep concrete flume of Universidade da Beira Interior described by Lança et al. (2013), and adopting their experimental procedure. Depending on the experiment, the flume was narrowed to 2.00 or 1.50 m to guarantee combinations of sufficiently high average approach flow velocity and flow depth.

Eight experiments were performed (two sets of four experiments per set). Four piers, simulated by PVC pipes with D_p = [50,75,150,175] mm, were used. Two experiments were made per pier (one per set), embedded in the same uniform quartz sand ($\rho_s = 2660\ \mathrm{kg/m^3}$; submerged relative density $\Delta \approx 1.66$ constant), by imposing two different flow depths so that d/D_p = [1.0,1.5]. Sand mixtures were obtained so as to keep d/D_{50} constant within each set. The values of D_{50} and σ_D corresponding to piers D_p = [50,75,150,175] mm were, respectively, D_{50} = [0.86,1.28,2.56,3.00] mm and σ_D = [1.36,1.50,1.18,1.26]. The average approach flow velocity, U, was computed so as to keep F_{50} constant. Experiments lasted for at least 7 days, which guarantees sufficient approximation to the equilibrium stage.

Results and Discussion

The flume width, W, sediment size, D_{50}, pier diameter, D_p, flow depth, d, approaching mean flow velocity, U, and some relevant viscous-independent dimensionless groups are shown in Table 1 for each of the eight experiments. The dimensionless groups are the aforementioned d/D_{50}, d/D_p and F_{50} — required to be constant within each set, recalling Eqs. (8), (9), and (11) — and W/d, W/D_p, and the flow Froude number F_d (=$U/\sqrt{gd}$). A constant in all the experiments is $D_p/D_{50} \sim 58$.

From Table 1 it can be concluded that (1) reasonably high relative flow depth—d/D_{50} = [58,87]—was always guaranteed; (2) the aspect ratio varied in the range $5.7 \leqslant W/d \leqslant 53.3$, this way avoiding significant wall effects on the flow field; (3) the ratio of channel width to pier diameter, W/D_p, was at least 8.6, close enough to $W/D_p = 10$, above which contraction effects are absent, and on these effects, it must also be noted that no measurable bed degradation was registered over the contracted cross section; and (4) except for W/d and W/D_p, whose influence can be neglected, the four tests within each set respect the Froude similarity.

The viscosity (which changed from test to test because of the changes in the water temperature) and some viscous-dependent dimensionless groups are shown in Table 2. The water temperature was measured for all the experiments except for Set1-1 and Set2-1. However, because these experiments were run in a period of the year in which the water temperature in the laboratory is known to vary between 15 and 20°C, it was assumed to be 17.5°C.

The critical velocity, U_c, employed to obtain $\mathcal{J}$, is computed as follows. First, the critical shear velocity is $u_{*c} = \sqrt{g\Delta D_{50}\tau_{*c}}$ and the critical shear stress is $\tau_c = \rho u_{*c}^2$, where τ_{*c} is the critical value of Shields parameter, obtained here from d_* as

Table 1. Experimental Conditions and Viscous Independent Dimensionless Groups

Test	W (mm)	D_{50} (mm)	D_p (m)	d(m)	U (m/s)	d/D_{50} (–)	d/D_p (–)	F_{50} (–)	W/d (–)	W/D_p (–)	F_d (–)
Set 1-1	2.0	0.86	0.050	0.050	0.272	58.1	1.00	2.30	40.0	40.0	0.39
Set 1-2	4.0	1.28	0.075	0.075	0.333	58.6	1.00	2.31	53.3	53.3	0.39
Set 1-3	1.5	2.56	0.150	0.150	0.470	58.6	1.00	2.30	10.0	10.0	0.39
Set 1-4	1.5	3.00	0.175	0.175	0.509	58.3	1.00	2.30	8.6	8.6	0.39
Set 2-1	2.0	0.86	0.050	0.075	0.284	87.2	1.50	2.40	26.7	40.0	0.33
Set 2-2	4.0	1.28	0.075	0.113	0.347	88.3	1.51	2.40	35.4	53.3	0.33
Set 2-3	1.5	2.56	0.150	0.225	0.490	87.9	1.50	2.40	6.7	10.0	0.33
Set 2-4	1.5	3.00	0.175	0.263	0.530	87.7	1.50	2.40	5.7	8.6	0.33

Table 2. Viscosity, Viscous Dependent Groups and Equilibrium Scour

Test	ν (mm^2/s)	d_* (–)	τ_{*c} (–)	$\mathcal{J}$ (–)	R_p (–)	R_s (–)	k_s^+ (–)	B_* (–)	d_{se}(m)	d_{se}/D_p (–)
Set 1-1	1.080	20.7	0.0303	0.779	0.13×10^5	0.22×10^3	12.7	9.5	0.116	2.32
Set 1-2	1.065	31.1	0.0336	0.757	0.23×10^5	0.40×10^3	23.9	9.2	0.165	2.20
Set 1-3	0.996	65.1	0.0449	0.689	0.71×10^4	1.21×10^3	76.1	8.6	0.263	1.75
Set 1-4	0.923	80.2	0.0482	0.670	0.97×10^5	1.65×10^3	105.3	8.6	0.296	1.69
Set 2-1	1.080	20.7	0.0303	0.770	0.13×10^5	0.23×10^3	12.5	9.5	0.119	2.38
Set 2-2	1.130	29.9	0.0332	0.749	0.23×10^5	0.39×10^3	22.1	9.2	0.170	2.27
Set 2-3	0.994	65.1	0.0449	0.682	0.74×10^5	1.26×10^3	75.6	8.6	0.296	1.97
Set 2-4	0.923	80.2	0.0482	0.664	1.00×10^5	1.72×10^3	104.4	8.6	0.324	1.85

$$\tau_{*c} = 0.24/d_* + 0.055[1 - \exp(-d_*^{1.05}/58)] \quad (12)$$

This expression is an approximation of the more complex expression proposed by Hoffmans and Verheij (1997). We remark that d_* ranged from ~20 to ~80 so that the viscosity has an influence on sediment entrainment (τ_{*c} ranges from ~0.030 to ~0.048).

Once the critical shear velocity u_{*c} and the critical shear stress τ_c are known, critical depth averaged velocity is $U_c = \sqrt{\tau_c/(\rho C_f)}$, where the friction coefficient, C_f, can be obtained by integrating the law of the wall. For $d \gg k_s$, with $k_s \sim D_{50}$ the equivalent roughness, C_f reads

$$C_f = \left(\kappa^{-1} \ln \frac{R}{e z\text{min}}\right)^{-2} \quad (13)$$

with e = Euler number; $\kappa \sim 0.4$ (von Karman's constant); $R \equiv Wd/(W + 2d)$ is the hydraulic radius; and $z$min = distance above the bed where the velocity cancels, which is given by $z\,\text{min} = k_s \exp(-\kappa B_*)$, where B_* is obtained from $k_s^+ \equiv u_* k_s/\nu$ using the equation

$$B* = -\ln((9k_s^+)^{-\kappa^{-1}} + 2.034 \cdot 10^{-4}\{1 - \exp[-0.0368(k_s^+)^{0.921}]\}) \quad (14)$$

This expression is an approximation of the experimental data for B_* (Fig. 1) obtained by Nikuradse and reproduced by Yalin (1972). Moreover, from Eq. (14) one automatically recovers the well known expressions for the rough and smooth limiting cases: for large k_s^+ (rough boundary layer), it tends to $B_* = 8.5$, and for small k_s^+ (smooth boundary layer), it tends to $B_* = \kappa^{-1} \ln k_s^+ + 5.5$.

Recall that, to obtain U_c, one must consider critical conditions, *i.e.*, $k_s^+ = u_{*c} k_s/\nu$ with $u_{*c} = \sqrt{g\Delta \mathrm{D}_{50} \tau_{*c}}$ to compute B_*, z min and C_f.

Notice that U_c depends on the viscosity in two different ways: through the mobility of the sediment (τ_{*c} depends on d_*, *i.e.*, on the viscosity) and through the resistance equation (because z min depends on the viscosity). However, the influence through τ_{*c} seems to be much stronger than through z min. Using the previous expressions, if one disregards the effect of viscosity through τ_{*c} (i.e., setting $\tau_{*c} = 0.055$, the value for large d_*), the changes in U_c are around one order of magnitude bigger than those obtained if one disregards the effects of the viscosity through $z$min (i.e., setting $B_* = 8.5$ and $z\text{min} = k_s \exp(-\kappa B_*) \sim k_s/30$).

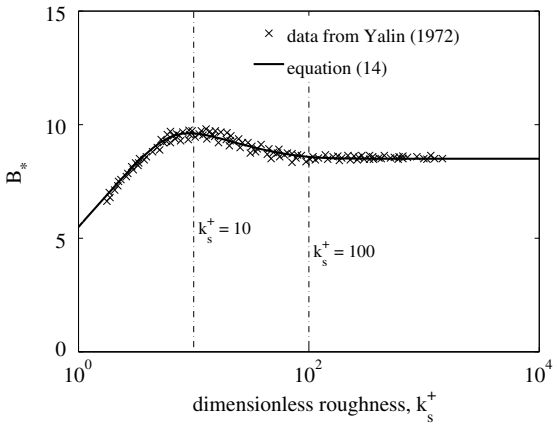

Fig. 1. Resistance equation B* = f(k_s^+)

Table 2 includes relevant viscous-dependent dimensionless groups such as the dimensionless diameter d_*, the critical Shields parameter τ_{*c} obtained through Eq. (12), the flow intensity $\mathcal{J}$, and Reynolds numbers R_p and R_s. It also includes $k_s^+ = u_* k_s/\nu$ and B_*, obtained iteratively from the actual flow conditions (U, d) using Eqs. (13) and (14). Dimensionless roughness k_s^+ ranges from 13 to 105 in the experiments so that, according to Fig. 1, the approaching flow is transitional, *i.e.*, viscous effects are not negligible. (There is a viscous sublayer within the boundary layer.)

Finally, Table 2 includes the equilibrium scour depth, d_{se}, and d_{se}/D_p. Because the experiments lasted at least seven days, d_{se} was obtained by extrapolating the scour-depth time records to $t \to \infty$ through the six parameters polynomial function suggested by Lança et al. (2010).

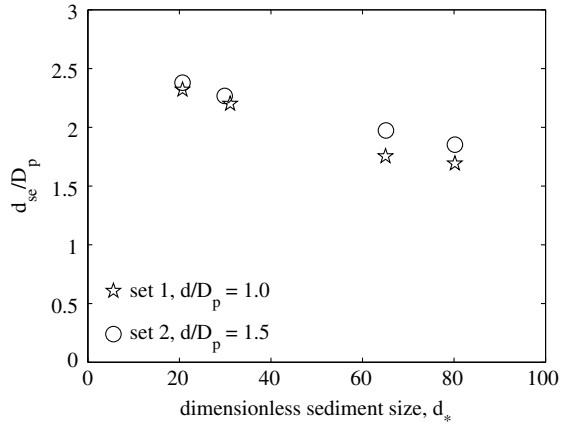

Fig. 2. Viscous effects on dse/Dp

Influence of the Viscosity on Local Scour

Recalling, e.g., Eq. (9), Fig. 2 shows the variation of the dimensionless scour depth, d_{se}/D_p with d_*. To no surprise, the figure shows a slight increase of the dimensionless scour depth as d/D_p changes from 1.0 to 1.5. Remarkably, it also shows that, within each set (where d/D_{50}, d/D_p and F_{50} are constant, and only d_* varies), the dimensionless scour depth decreases with d_*. This demonstrates that viscous effects influence scouring, *i.e.*, that ν has an influence on d_{se}. Naturally, the same conclusion is drawn within the framework of Eqs. (8) and (11) and using the data in Table 2. This corroborates some early results by Shen et al. (1969), and the trends reported by Nicollet and Ramette (1971). We emphasize that in Eq. (8), where the velocity is also included in F_{50}, $\mathcal{I}$ plays a role as representative of the viscosity. In fact, considering the framework given by Eq. (8), $\mathcal{I}$ would be constant if the viscosity were not to have an influence on the upstream flow (rough turbulent) nor on the Shields parameter ($d_* \geqslant 150$).

The aforementioned results confirm that, at least for the two terns of d/D_{50}, d/D_p, and F_{50} considered in sets 1 and 2, and for the given ranges of variation of d_*, the viscosity has an influence on the local scour phenomena. As it happens in the upstream flow, this influence is expected to have two components: through the Shields' parameter for the sediment entrainment (τ_{*c}) and also through the development of a viscous sublayer in the boundary layer. If the influence was driven, as it happens in the upstream flow, primarily through the Shields parameter τ_{*c}, then the relationship d_{se}/D_p against τ_{*c} could be of interest. Using τ_{*c} computed from d_* using Eq. (12), it is shown from Table 2 that the scour depth d_{se}/D_p decreases as the τ_{*c} increases (less mobility), which is in accordance with intuition.

Conclusions

The results of this study indicate that, contrary to a rather common assumption, scouring does depend on viscosity in usual laboratory conditions. The viscous effects being present in local scour phenomena has consequences in the physical modeling of bridge scour. In usual hydraulic problems that do not involve sediment transport, viscous effects are often neglected and Froude similarity is used, leaving open the possibility of Reynolds-type scale effects. Bridge scour problems, which involve sediment transport, add another difficulty: the geometric similarity is frequently broken because it is, in practice, impossible to keep D_p/D_{50} with the same value in prototype and in the laboratory. The experimental results obtained here show that Reynolds-type scale effects appear in the physical modeling of local scour. According to the experimental results; however, the smaller the model (*i.e.*, the smaller d_*, or R_p), the bigger the nondimensional scour depth (d_{se}/D_p), so that the experimental results in laboratory yield results in the safety side. In view of the limited evidence of this study, further research is required to confirm this result. Further research should include the explanation of the viscosity effect throughout detailed flow mapping and modeling.

Acknowledgments

This work was partially funded by projects RECI/ECM-HID/0371/2012 [Fundo Europeu de Desenvolvimento Regional (FEDER), program Programa Operacional Factores de Competitividade (COMPETE), Portuguese Foundation for Science and Technology, Fundação para a Ciência e Tecnologia (FCT)] and PTDC / ECM / 101353 / 2008 (FCT). G. Simarro is supported by the Spanish government through the Ramón y Cajal program.

References

Coleman, N. L. (1971). "Analyzing laboratory measurements of scour at cylindrical piers in sand beds." *Proc., 14th IAHR Congress*, IAHR, Paris, 307–313.

Ettema, R., Kirkil, G., and Muste, M. (2006). "Similitude of large-scale turbulence in experiments on local scour at cylinders." *J. Hydraul. Eng.*, 10.1061/(ASCE)0733-9429(2006)132:1(33), 33–40.

Hoffmans, G. J. C. M., and Verheij, H. J. (1997). *Scour manual*, A.A. Balkema, Rotterdam, the Netherlands.

Lança, R., Fael, C., and Cardoso, A. (2010). *Assessing equilibrium clear-water scour around single cylindrical piers*, Bundesanstalt fur Wasserbau, Karlsruhe, Germany, 1207–1213.

Lança, R., Fael, C., Maia, R., Pego, J. P., and Cardoso, A. (2013). "Clear-water scour at comparatively large cylindrical piers." *J. Hydraul. Eng.*, 10.1061/(ASCE)HY.1943-7900.0000788, 1117–1125.

Monti, R. (1994). *Indagine sperimentale delle caratteristiche fluidodinamiche del campo di moto intorno a una pila circolare*, Polytechnic of Milan, Milan, Italy (in Italian).

Nicollet, G., and Ramette, M. (1971). *Deformation des lits alluvionnaires affouillements autour des piles de ponts cylindriques*, Direction des Etudes et Recherches (EDF), Chatou, France (in French).

Shen, H. W., Schneider, V. R., and Karaki, S. S. (1969). "Local scour around bridge piers." *J. Hydraul. Div.*, 95(HY6), 1919–1940.

Simarro, G., Teixeira, L., and Cardoso, A. H. (2007). "Flow intensity parameter in pier scour experiments." *J. Hydraul. Eng.*, 10.1061/(ASCE)0733-9429(2007)133:11(1261), 1261–1264.

Yalin, M. S. (1972). *Mechanics of sediment transport*, Pergamon Press, Oxford, England.